

## SUPPLEMENTARY MATERIAL

**“Further extension of the Madrid–2019 force field: Parametrization of the nitrate ( $\text{NO}_3^-$ ) and ammonium ( $\text{NH}_4^+$ ) ions. ”.**

Víctor M. Trejos<sup>1,2†</sup>, Marcos de Lucas<sup>2†</sup>, Carlos Vega<sup>2</sup>, Samuel Blazquez<sup>2,\*</sup>, Francisco Gámez<sup>2,\*</sup>

<sup>1</sup>Departamento de Química, Universidad Autónoma Metropolitana-Iztapalapa,  
Av. San Rafael Atlixco 186, Col. Vicentina, 09340, Ciudad de México, Mexico.

<sup>2</sup>Departamento de Química Física, Universidad Complutense de Madrid, 28040 Madrid, Spain.

<sup>†</sup>These authors contributed equally to this work.

\*Corresponding authors: samuelbl@ucm.es, frgamez@ucm.es

The Supplementary Material for the publication ‘Further extension of the Madrid–2019 library: Parametrization of the  $\text{NO}_3^-$  and  $\text{NH}_4^+$  ions’ contains the compilation of the numerical (raw data) and graphical information of the simulation results of all nitrate and ammonium salts considered in the main body of this work for the following properties:

- The results for the Lennard-Jones energy parameters,  $\sigma_{ij}$  and  $\varepsilon_{ij}$  of the force field.
- Simulation results for the density ( $\rho^{\text{sim}}$ ) as a function of the molality ( $m$ ). The experimental data ( $\rho^{\text{exp}}$ ) were obtained from Refs.[1–3], for most salts but for  $\text{RbNO}_3$  and  $\text{CsNO}_3$ , for which the values were extracted from Ref.[4] and Ref.[5], respectively.
- Same as previous bullet but for experimental ( $\eta^{\text{exp}}$ ) and simulated ( $\eta^{\text{sim}}$ ) shear viscosities. In this case, all experimental data were obtained from Refs.[1–3].
- The simulated atom-atom RDFs of interest for the whole set of electrolyte aqueous solutions considered in this work. We include a schematic representation of the expected RDFs pattern for different type of ion–ion arrangements and of the geometrical features of the  $\text{NO}_3^-$  and  $\text{NH}_4^+$  ions.

Unless otherwise mentioned, the reported data correspond to a thermodynamic state at 298.15 K and 1 bar.

## I. COMPLEMENTARY TABLES

Table S I. Lennard–Jones  $\sigma_{ij}$  parameters (in Å) of the proposed force field.

Atom	$N_n$	$O_n$	$N_a$
$O_w$	3.1545	3.2300	3.0540
$Li^+$	2.2949	3.3000	2.3449
$Na^+$	2.6837	3.0000	2.7337
$K^+$	2.7257	3.3000	2.7757
$Rb^+$	3.0725	3.2000	3.1225
$Cs^+$	3.3355	3.4000	3.3855
$Mg^{2+}$	2.1565	3.4000	2.2065
$Ca^{2+}$	2.9078	2.7628	2.9578
$N_a$	3.9000	3.0550	*
$F^-$	3.4699	3.3249	3.5400
$Cl^-$	3.9245	3.7795	3.9745
$Br^-$	3.9876	3.8426	4.0376
$N_n$	*	3.0050	3.9000
$O_n$	3.0050	*	3.0550
S	3.3500	3.2050	3.4000
$O_S$	3.4000	3.2550	3.3000

\*These values are reported in Table I of the manuscript.

Table S II. Lennard–Jones  $\varepsilon_{ij}$  parameters (in kJ/mol) obtained from the LB rules.

Atom	$N_n$	$O_n$	$N_a$
$O_w$	0.7423	0.8248	0.7423
$Li^+$	0.5562	0.6181	0.5562
$Na^+$	1.0232	1.1369	1.0232
$K^+$	1.1882	1.3204	1.1882
$Rb^+$	1.1507	1.2787	1.1507
$Cs^+$	0.5170	0.5745	0.5170
$Mg^{2+}$	1.6114	1.7906	1.6114
$Ca^{2+}$	0.6005	0.6673	0.6005
$N_a$	0.7110	0.7901	0.7110
$F^-$	0.1484	0.1649	0.1484
$Cl^-$	0.2339	0.2599	0.2339
$Br^-$	0.2832	0.3147	0.2832
$N_n$	0.7110	0.7901	0.7110
$O_n$	0.7901	0.8780	0.7901
S	0.8627	0.9586	0.8627
$O_S$	0.7716	0.8575	0.7716

## II. RAW DATA

### A. Bulk densities

Table S III. Comparison between simulation results and experimental data for the bulk density variation with molality for  $\text{LiNO}_3$ ,  $\text{NaNO}_3$ , and  $\text{KNO}_3$ . Experimental data were obtained from Refs.[1–3]. The relative percentage deviation is given by  $\text{dev.}(\%) = 100 \times |\rho^{\text{exp}} - \rho^{\text{sim}}| / \rho^{\text{exp}}$ . Units in mol/kg for  $m$  and  $\text{kg/m}^3$  for density.

$\text{LiNO}_3$				$\text{NaNO}_3$				$\text{KNO}_3$			
$m$	$\rho^{\text{exp}}$	$\rho^{\text{sim}}$	dev.(%)	$m$	$\rho^{\text{exp}}$	$\rho^{\text{sim}}$	dev.(%)	$m$	$\rho^{\text{exp}}$	$\rho^{\text{sim}}$	dev.(%)
0.000	997.05	997.30	0.02	0.00	997.05	997.30	0.03	0.00	997.05	997.30	0.03
1.00	1035.32	1032.45	0.28	1.00	1050.00	1050.08	0.07	0.50	1027.20	1027.03	0.02
2.00	1069.91	1065.11	0.45	2.00	1098.00	1097.59	0.04	1.00	1055.30	1055.38	0.01
3.00	1103.06	1095.73	0.66	3.00	1140.90	1141.34	0.04	2.00	1107.60	1107.39	0.02
4.00	1133.66	1124.27	0.83	4.00	1182.00	1181.33	0.06	3.00	1154.40	1153.95	0.04
5.00	1161.80	1151.48	0.89	5.00	1219.10	1218.16	0.08	4.00	--	1196.18	--
6.00	1189.58	1177.14	1.05	6.00	1254.40	1252.51	0.15				
8.00	1239.47	1224.34	1.22	8.00	1316.04	1313.45	0.20				
10.0	1282.68	1267.60	1.18	10.0	1369.38	1366.16	0.24				
12.0	1321.27	1307.82	1.02								
14.0	1358.20	1348.29	0.72								

Table S IV. The same as in Table SIII but for  $\text{RbNO}_3$  and  $\text{CsNO}_3$ . The experimental information were extracted from Ref.[4] and Ref.[5] for  $\text{RbNO}_3$  and  $\text{CsNO}_3$ , respectively.

$\text{RbNO}_3$				$\text{CsNO}_3$			
$m$	$\rho^{\text{exp}}$	$\rho^{\text{sim}}$	dev.(%)	$m$	$\rho^{\text{exp}}$	$\rho^{\text{sim}}$	dev.(%)
0.00	997.05	997.30	0.03	0.00	997.05	997.30	0.03
1.00	1090.76	1089.64	0.10	0.20	1025.40	1025.31	0.01
2.00	1175.28	1172.87	0.20	0.50	1066.62	1065.43	0.11
3.00	1250.48	1248.75	0.14	1.00	1132.11	1129.35	0.24
4.00	1316.84	1317.42	0.04				

Table S V. The same as in Table SIII but for  $\text{Mg}(\text{NO}_3)_2$  and  $\text{Ca}(\text{NO}_3)_2$ . The experimental data for  $\text{Mg}(\text{NO}_3)_2$  and  $\text{Ca}(\text{NO}_3)_2$  were obtained from Refs.[1–3].

$\text{Mg}(\text{NO}_3)_2$				$\text{Ca}(\text{NO}_3)_2$			
$m$	$\rho^{\text{exp}}$	$\rho^{\text{sim}}$	dev.(%)	$m$	$\rho^{\text{exp}}$	$\rho^{\text{sim}}$	dev.(%)
0.00	997.05	997.30	0.03	0.00	997.05	997.30	0.03
1.00	1098.80	1094.95	0.35	1.00	1108.10	1108.60	0.05
2.00	1187.00	1181.75	0.44	2.00	1204.34	1204.00	0.03
3.00	1263.90	1259.75	0.33	3.00	1288.86	1285.90	0.23
4.00	1328.60	1329.72	0.09	4.00	1358.00	1356.23	0.13
5.00	1394.17	1393.00	0.08	5.00	1420.83	1415.50	0.38
				6.00	1475.94	1468.04	0.54
				7.00	1524.91	1513.72	0.73
				8.00	1568.19	1557.24	0.70
				9.00	1606.83	1601.28	0.35
				10.0	1641.34	1639.10	0.14

Table S VI. The same as in Table SIII but for  $\text{NH}_4\text{F}$ ,  $\text{NH}_4\text{Cl}$ , and  $\text{NH}_4\text{Br}$ . Experimental data for  $\text{NH}_4\text{F}$  and  $\text{NH}_4\text{Br}$  were extracted from Refs.[6] and from Ref.[1–3] for  $\text{NH}_4\text{Cl}$ . In the case of  $\text{NH}_4\text{F}$ , the experimental data were measured and simulated at 291.15 K and 1 bar.

$\text{NH}_4\text{F}$				$\text{NH}_4\text{Cl}$				$\text{NH}_4\text{Br}$			
$m$	$\rho^{\text{exp}}$	$\rho^{\text{sim}}$	dev.(%)	$m$	$\rho^{\text{exp}}$	$\rho^{\text{sim}}$	dev.(%)	$m$	$\rho^{\text{exp}}$	$\rho^{\text{sim}}$	dev.(%)
0.00	997.05	997.30	0.03	0.00	997.05	997.30	0.03	0.00	997.05	997.30	0.03
1.00	1015.77	1017.45	0.17	0.50	1005.12	1005.10	0.00	1.00	1048.83	1048.10	0.07
2.00	1030.09	1032.43	0.23	1.00	1012.65	1012.50	0.01	2.00	1094.96	1094.08	0.08
3.00	1042.00	1044.44	0.23	2.00	1025.87	1025.88	0.00	3.00	1137.29	1136.08	0.11
4.00	1051.38	1054.64	0.31	3.00	1037.81	1038.00	0.02	4.00	1176.04	1174.12	0.16
5.00	—	1063.18	—	4.00	1048.63	1048.92	0.03	5.00	1211.69	1209.56	0.18
				5.00	1057.80	1058.55	0.07	7.00	1276.34	1271.65	0.37
				7.00	1077.30	1075.02	0.21				

Table S VII. The same as in Table SIII but for  $(\text{NH}_4)_2\text{SO}_4$  and  $\text{NH}_4\text{NO}_3$ . Experimental data for  $\text{NH}_4\text{SO}_4$  and  $\text{NH}_4\text{NO}_3$  were obtained from Refs.[1–3].

$(\text{NH}_4)_2\text{SO}_4$				$\text{NH}_4\text{NO}_3$				$\text{NH}_4\text{NO}_3, T = 323.15 \text{ K}$			
$m$	$\rho^{\text{exp}}$	$\rho^{\text{sim}}$	dev.(%)	$m$	$\rho^{\text{exp}}$	$\rho^{\text{sim}}$	dev.(%)	$m$	$\rho^{\text{exp}}$	$\rho^{\text{sim}}$	dev.(%)
0.00	997.05	997.30	0.03	0.00	997.05	997.30	0.03	2.00	1042.68	1040.30	0.23
1.00	1065.00	1066.06	0.09	1.00	1027.16	1026.16	0.10	5.00	1105.95	1103.23	0.25
2.00	1117.70	1118.92	0.11	2.00	1053.53	1052.79	0.01	10.0	1180.64	1178.47	0.18
3.00	1160.70	1161.68	0.08	5.00	1119.04	1119.61	0.05				
4.00	1197.34	1196.30	0.09	8.00	1168.13	1170.11	0.16				
5.00	1225.29	1225.09	0.02	12.0	1220.40	1220.39	0.00				
6.00	1250.18	1249.25	0.07	16.0	1255.09	1256.95	0.15				
				20.0	1284.16	1284.65	0.04				
				26.0	1318.77	1314.79	0.30				

## B. Shear viscosities

Table S VIII. Comparison between simulation results and experimental data for shear viscosity variation with molality for  $\text{NaNO}_3$ ,  $\text{KNO}_3$ ,  $\text{RbNO}_3$ , and  $\text{CsNO}_3$ . Experimental data were obtained from Refs.[1–3]. The viscosity of the TIP4P/2005 model is 0.85(5) mPa·s, according to Ref.[7], and the experimental data is 0.89 mPa·s [8]. The relative percentage deviation is given by  $\text{dev.}(\%) = 100 \times |\eta^{\text{exp}} - \eta^{\text{sim}}|/\eta^{\text{exp}}$ . Units in mol/kg for  $m$  and mPa·s for shear viscosity  $\eta$ .

$\text{NaNO}_3$				$\text{KNO}_3$				$\text{RbNO}_3$				$\text{CsNO}_3$			
$m$	$\eta^{\text{exp}}$	$\eta^{\text{sim}}$	dev.(%)	$m$	$\eta^{\text{exp}}$	$\eta^{\text{sim}}$	dev.(%)	$m$	$\eta^{\text{exp}}$	$\eta^{\text{sim}}$	dev.(%)	$m$	$\eta^{\text{exp}}$	$\eta^{\text{sim}}$	dev.(%)
2.00	1.03	0.95(5)	7.77	1.00	0.87	0.83(4)	4.60	2.00	0.85	0.86(3)	1.18	0.50	0.86	0.87(3)	1.16
4.00	1.26	1.23(7)	2.38	3.00	0.92	0.85(4)	7.61	3.00	0.87	0.90(3)	3.44	1.00	0.84	0.83(5)	1.19
								4.00	0.91	0.93(5)	2.20	1.50	--	0.82(9)	--

Table S IX. The same as in Table VIII but for  $\text{CsNO}_3$ ,  $\text{NH}_4\text{Cl}$ , and  $\text{NH}_4\text{NO}_3$ . Experimental data were obtained from Ref.[1–3]. The viscosity of the TIP4P/2005 model is 0.85(5) mPa·s, according to Ref.[7], and the experimental data is 0.89 mPa·s [8].

$\text{NH}_4\text{NO}_3$				$(\text{NH}_4)_2\text{SO}_4$				$\text{NH}_4\text{Cl}$			
$m$	$\eta^{\text{exp}}$	$\eta^{\text{sim}}$	dev.(%)	$m$	$\eta^{\text{exp}}$	$\eta^{\text{sim}}$	dev.(%)	$m$	$\eta^{\text{exp}}$	$\eta^{\text{sim}}$	dev.(%)
3.00	0.87	0.85(3)	2.30	1.00	1.08	0.98(5)	9.25	2.00	0.88	1.06(7)	20.45
5.00	0.91	0.95(4)	4.40	3.00	1.61	1.43(5)	11.18	4.00	0.89	1.32(6)	48.31
				5.00	2.33	2.13(10)	8.58				

## III. FIGURES

## A. Bulk densities

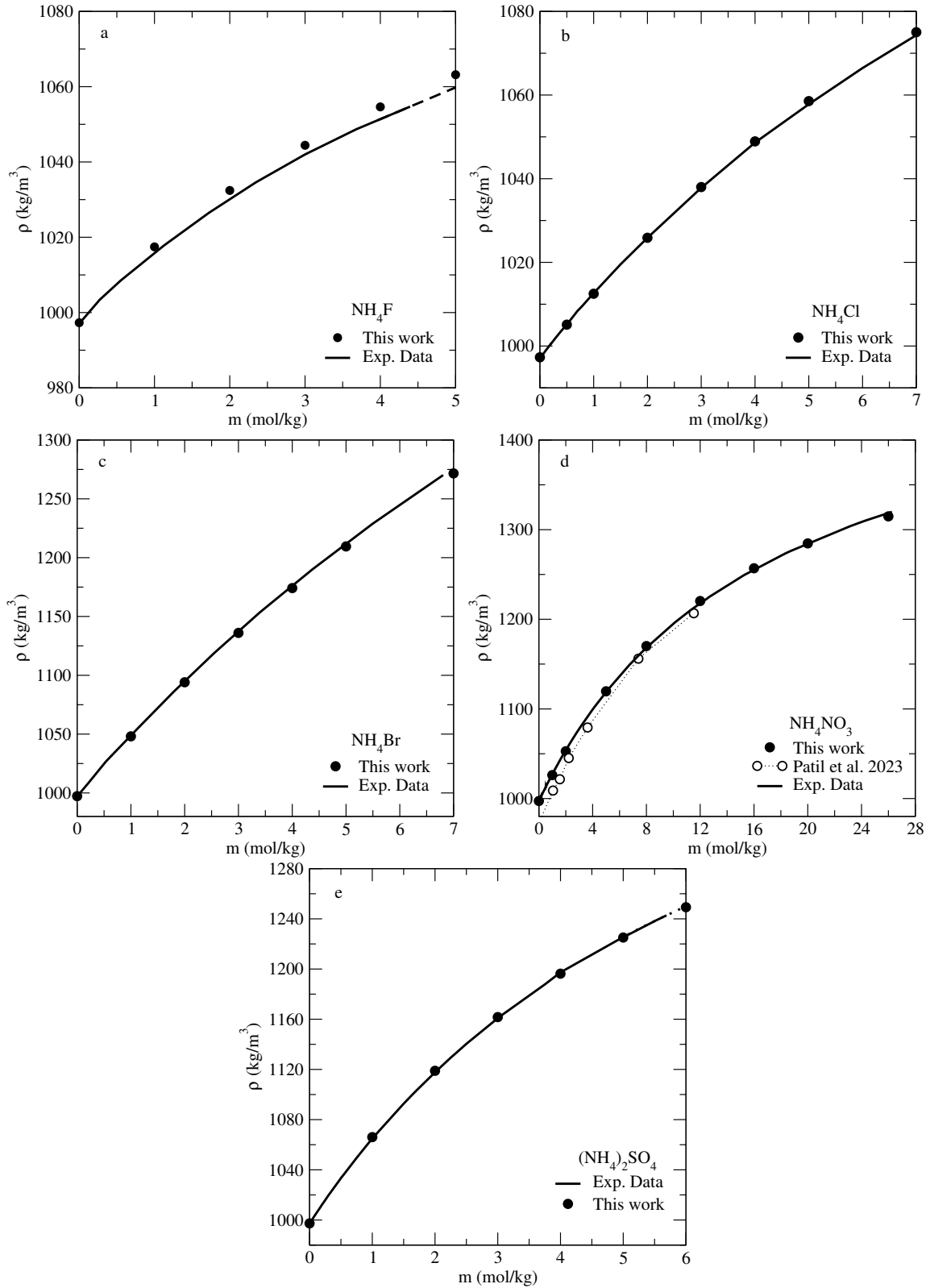


Fig. S 1. Panel (a): Density as a function of the molality for aqueous  $\text{NH}_4\text{F}$  solutions at 291.15 K and 1 bar. Panels (b) – (e): The same as in panel (a) but for  $\text{NH}_4\text{Cl}$ ,  $\text{NH}_4\text{Br}$ ,  $\text{NH}_4\text{NO}_3$ , and  $(\text{NH}_4)_2\text{SO}_4$ , respectively, at 298.15 K and 1 bar. The MD results are shown with filled circles, while continuous lines stand for the experimental data. These data are obtained for all salts from Refs.[1–3], and from Ref.[6] for  $\text{NH}_4\text{F}$ . In the case of  $\text{NH}_4\text{NO}_3$  simulation data results from Ref.[9] were included for comparison as empty circles.

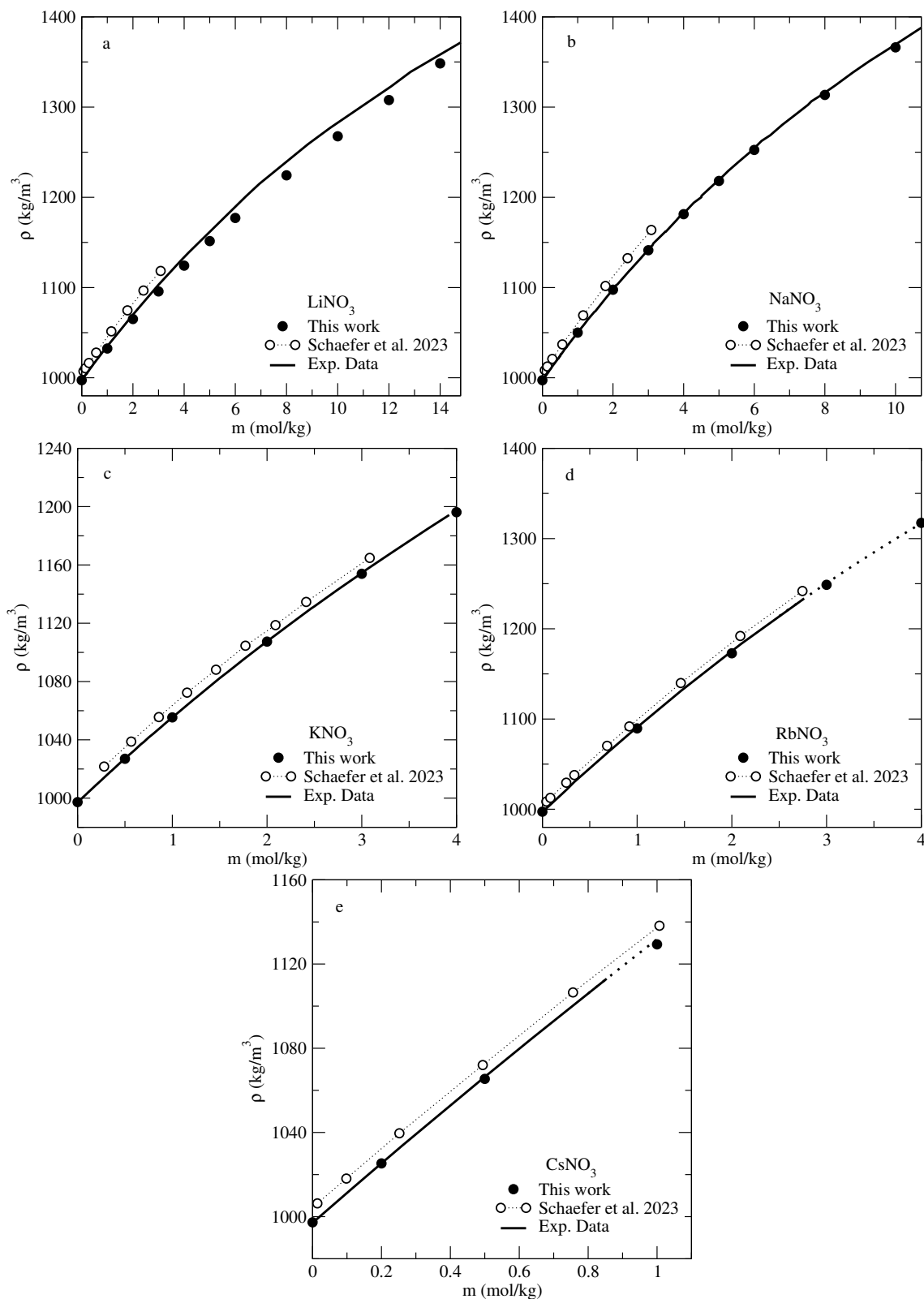


Fig. S 2. Panel (a): Density as a function of the molality for aqueous LiNO<sub>3</sub> solutions. Panel (b) – (e): The same as in panel (a), but for NaNO<sub>3</sub>, KNO<sub>3</sub>, RbNO<sub>3</sub>, and CsNO<sub>3</sub>, respectively. The MD results obtained from this work are shown with filled circles, while continuous lines stand for the experimental data. These data are obtained for all salts from Ref.[1–3] and from Refs.[4] and Ref.[5] for RbNO<sub>3</sub> and CsNO<sub>3</sub>, respectively. The empty circles are taken from Table S.III of the supplementary material of Ref.[10], and are included for comparison.

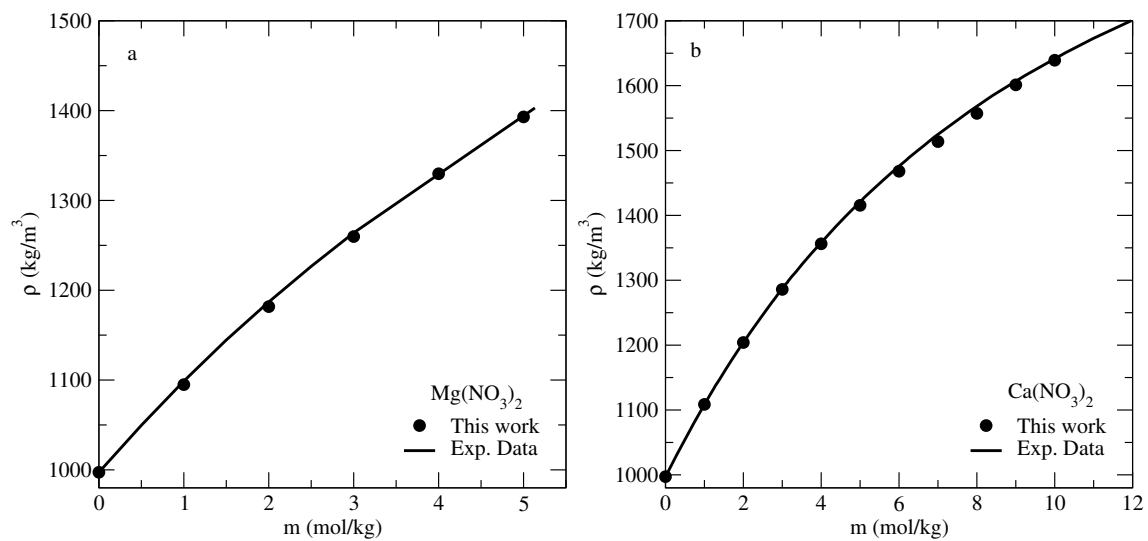


Fig. S 3. Panel (a): Density as a function of the molality for aqueous  $\text{Mg}(\text{NO}_3)_2$  solutions. Panel (b): The same as in panel (a) but for  $\text{Ca}(\text{NO}_3)_2$ . The MD results obtained from this work are shown with filled circles, while continuous lines stand for the experimental data from Refs.[1-3].

## B. Ion and solution structures

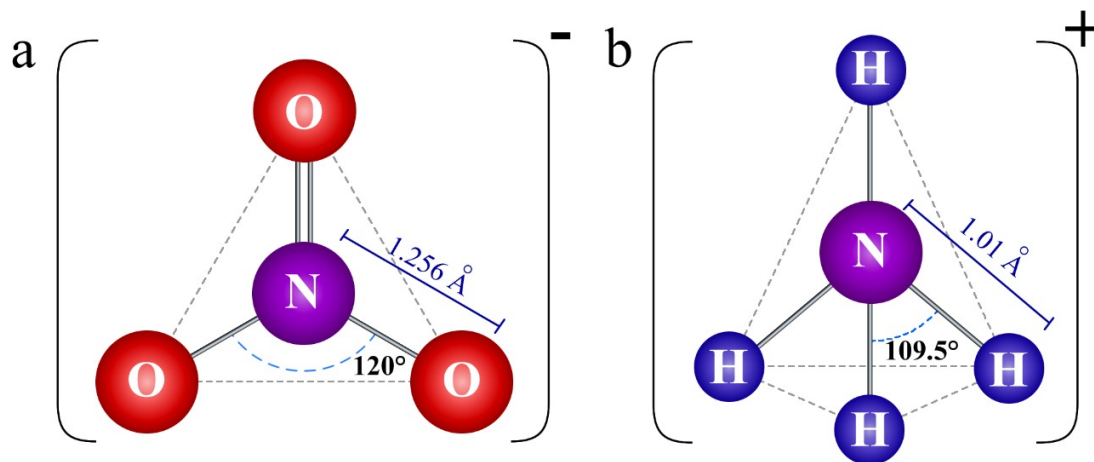
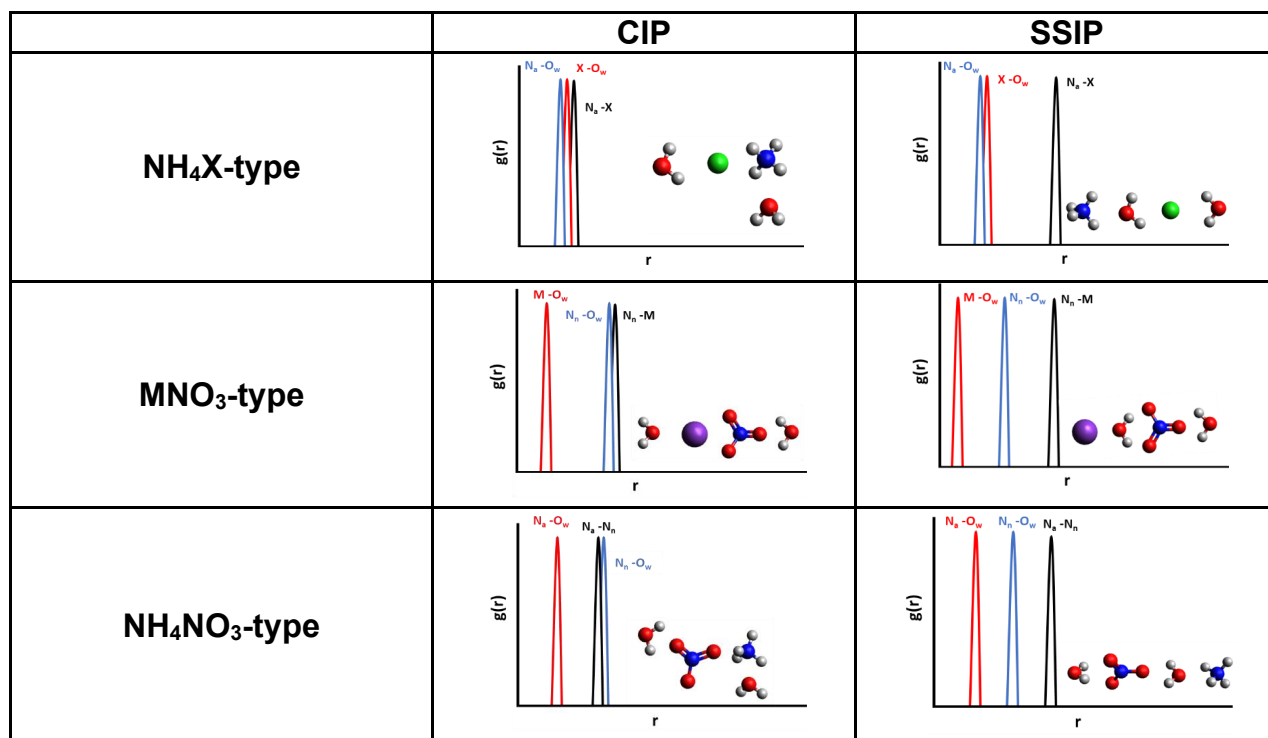


Fig. S 4. Geometrical model of the molecular (a) nitrate anion and (b) ammonium cation.

Fig. S 5. Schematic representation of the expected pattern of the RDFs of interest, *i.e.*, Cation-O<sub>w</sub>, anion-O<sub>w</sub> and anion-cation, for both SSIP and CIP arrangements. The inset shows an atomic 3D sketch of the atoms distributions in each case. The SSIP-type arrangement consists of at least one water molecule of separation between cation and anion.

## C. Radial distribution functions

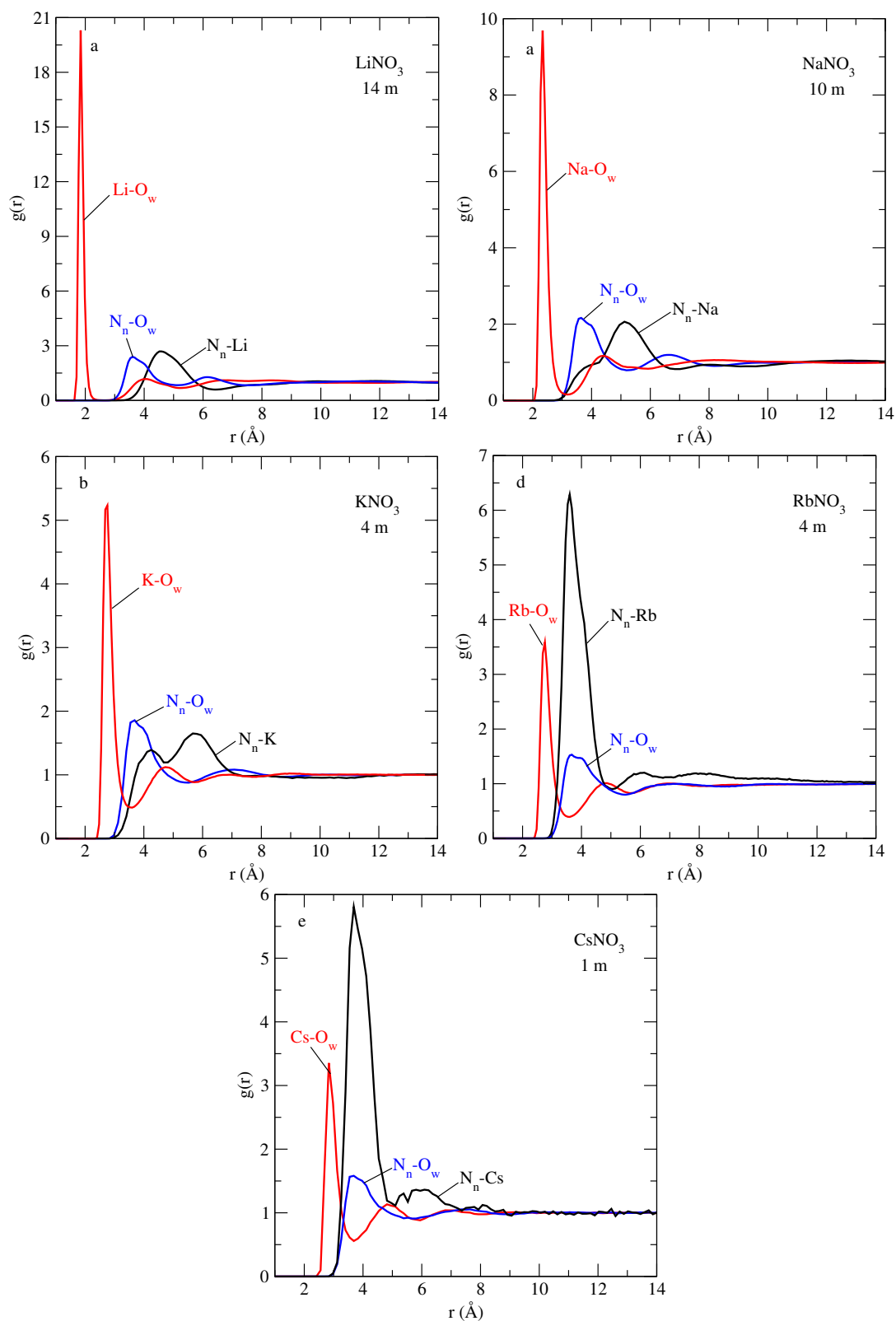


Fig. S 6. Panel (a): Cation- $\text{O}_w$  (red line),  $\text{N}_n\text{-O}_w$  (blue line) and  $\text{N}_n\text{-cation}$  (black line) radial distribution functions for aqueous  $\text{LiNO}_3$  solutions close to the solubility limit. Panel (b) - (e): The same as in panel (a) but for  $\text{NaNO}_3$ ,  $\text{KNO}_3$ ,  $\text{RbNO}_3$ , and  $\text{CsNO}_3$ , respectively.

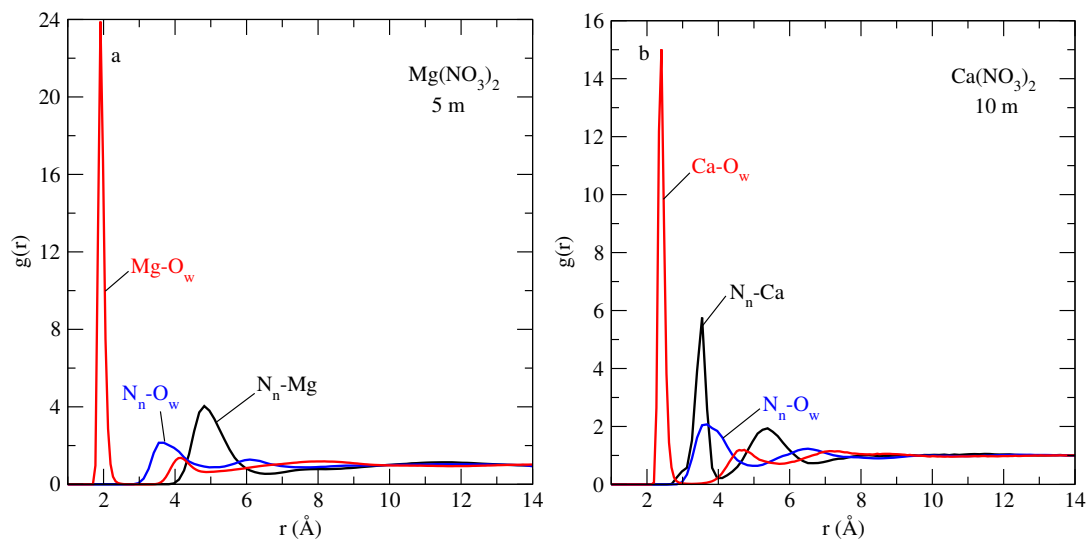


Fig. S 7. Panel (a): Cation- $\text{O}_w$  (red line),  $\text{N}_n$ - $\text{O}_w$  (blue line) and  $\text{N}_n$ -cation (black line) radial distribution functions for aqueous  $\text{Mg}(\text{NO}_3)_2$  solutions close to the solubility limit. Panel (b): Same as in panel (a) but for  $\text{Ca}(\text{NO}_3)_2$ .

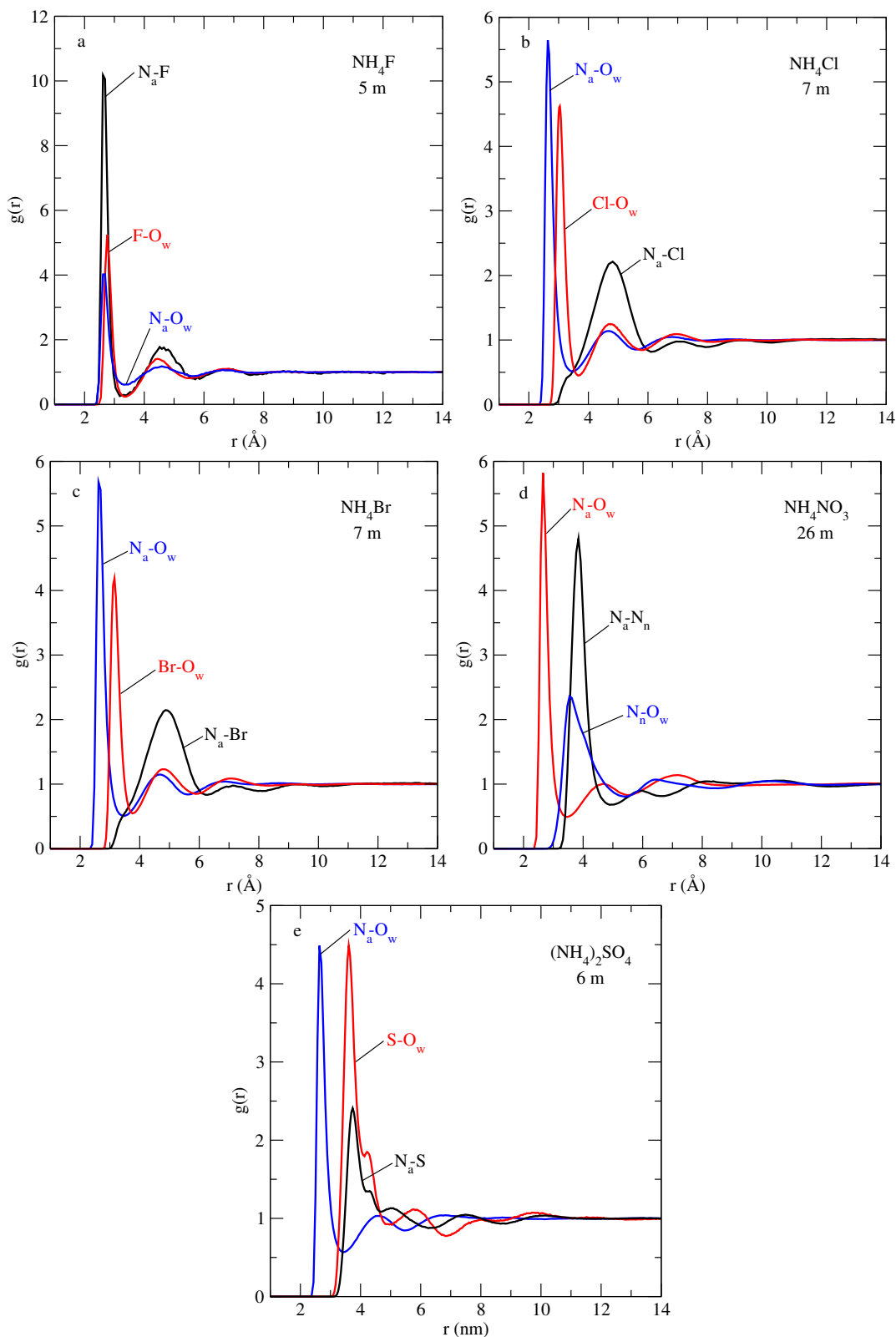


Fig. S 8. Panel (a): counterion- $\text{O}_w$  (red line),  $\text{N}_a\text{-O}_w$  (blue line) and  $\text{N}_a\text{-counterion}$  (black line) radial distribution functions for aqueous  $\text{NH}_4\text{F}$  solutions close to the solubility limit at 291.15 K and 1 bar. Panels (b) – (e): The same as in panel (a) but for  $\text{NH}_4\text{Cl}$ ,  $\text{NH}_4\text{Br}$ ,  $\text{NH}_4\text{NO}_3$ , and  $(\text{NH}_4)_2\text{SO}_4$ , respectively. In the case of  $\text{NH}_4\text{NO}_3$ , the ammonium is considered to be the counterion.

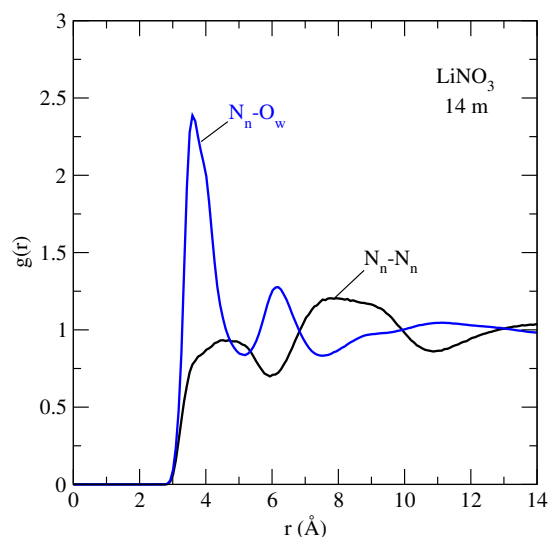


Fig. S 9.  $N_n$ - $O_w$  (blue line) and  $N_n$ - $N_n$  (black line) radial distribution functions for aqueous  $\text{LiNO}_3$  solutions 14 m. The overlapping between both RDFs indicates that running nitrate–nitrate contacts are non-negligible during the dynamics.

- 
- [1] M. Laliberte and W. E. Cooper, “Model for calculating the density of aqueous electrolyte solutions,” *J. Chem. Eng. Data*, vol. 49, no. 5, pp. 1141–1151, 2004.
- [2] M. Laliberte, “Model for calculating the viscosity of aqueous solutions,,” *J. Chem. Eng. Data*, vol. 52, no. 4, pp. 1507–1508, 2007.
- [3] M. Laliberte, “A model for calculating the heat capacity of aqueous solutions, with updated density and viscosity data,” *J. Chem. Eng. Data*, vol. 54, pp. 1725–1760, 2009.
- [4] H. G. Smith, J. H. Wolfenden, and H. Hartley, “LIV.-The viscosity and density of rubidium nitrate solutions,” *J. Chem. Soc.*, vol. 0, pp. 403–409, 1930.
- [5] T. R. Merton, “CCLIII - The viscosity and density of caesium nitrate solutions,” *J. Chem. Soc., Trans.*, vol. 97, pp. 2454–2463, 1910.
- [6] J. D’Ans, H. Surawski, and C. Synowietz, *Landolt-Bornstein. Numerical data and functional relationships in science and technology*. Springer-Verlag Berlin Heidelberg. New York, 1977.
- [7] S. Blazquez, M. M. Conde, J. L. F. Abascal, and C. Vega, “The Madrid-2019 force field for electrolytes in water using TIP4P/2005 and scaled charges: Extension to the ions  $\text{F}^-$ ,  $\text{Br}^-$ ,  $\text{I}^-$ ,  $\text{Rb}^+$ , and  $\text{Cs}^+$ ,” *J. Chem. Phys.*, vol. 156, p. 044505, 2022.
- [8] J. R. C. Jr. and T. B. Godfrey, “Viscosity of water,” *J. Applied Phys.*, vol. 15, pp. 625–626, 1944.
- [9] U. Patil and S. Keshri, “Unravelling the structural and dynamical properties of concentrated aqueous ammonium nitrate solutions: MD simulation studies,” *Mol. Sim.*, pp. 1–18, 2023.
- [10] D. Schaefer, M. Kohns, and H. Hasse, “Molecular modeling and simulation of aqueous solutions of alkali nitrates,” *J. Chem. Phys.*, vol. 158, pp. 134508(1)–134508(10), 2023.